Journal of Biomechanics 44 (2011) 669–675

Contents lists available at ScienceDirect

Journal of Biomechanics

journal homepage: www.elsevier.com/locate/jbiomech
www.JBiomech.com

# A simulation analysis of the combined effects of muscle strength and surgical tensioning on lateral pinch force following brachioradialis to flexor pollicis longus transfer

Jeremy P.M. Mogk [a,b,*], M. Elise Johanson [c], Vincent R. Hentz [c], Katherine R. Saul [d,e], Wendy M. Murray [a,b,f,g]

[a] Sensory Motor Performance Program, Rehabilitation Institute of Chicago, 345 E. Superior St., Chicago, IL 60611, USA
[b] Department of Physical Medicine & Rehabilitation, Northwestern University Feinberg School of Medicine, Chicago, IL, USA
[c] VA Palo Alto Health Care System, Palo Alto, CA, USA
[d] Department of Biomedical Engineering, Wake Forest University School of Medicine, Winston-Salem, NC, USA
[e] Virginia Tech-Wake Forest University School of Biomedical Engineering and Sciences, Winston-Salem, NC, USA
[f] Department of Biomedical Engineering, Northwestern University, Evanston, IL, USA
[g] Edward Hines, Jr. VA Hospital, Hines, IL, USA

ARTICLE INFO

*Article history:*
Accepted 2 November 2010

*Keywords:*
Biomechanical modeling
Simulation
Upper extremity
Lateral pinch
Upper limb function

ABSTRACT

Biomechanical simulations of tendon transfers performed following tetraplegia suggest that surgical tensioning influences clinical outcomes. However, previous studies have focused on the biomechanical properties of only the transferred muscle. We developed simulations of the tetraplegic upper limb following transfer of the brachioradialis (BR) to the flexor pollicis longus (FPL) to examine the influence of residual upper limb strength on predictions of post-operative transferred muscle function. Our simulations included the transfer, ECRB, ECRL, the three heads of the triceps, brachialis, and both heads of the biceps. Simulations were integrated with experimental data, including EMG and joint posture data collected from five individuals with tetraplegia and BR-FPL tendon transfers during maximal lateral pinch force exertions. Given a measured co-activation pattern for the non-paralyzed muscles in the tetraplegic upper limb, we computed the highest activation for the transferred BR for which neither the elbow nor the wrist flexor moment was larger than the respective joint extensor moment. In this context, the effects of surgical tensioning were evaluated by comparing the resulting pinch force produced at different muscle strength levels, including patient-specific scaling. Our simulations suggest that extensor muscle weakness in the tetraplegic limb limits the potential to augment total pinch force through surgical tensioning. Incorporating patient-specific muscle volume, EMG activity, joint posture, and strength measurements generated simulation results that were comparable to experimental results. Our study suggests that scaling models to the population of interest facilitates accurate simulation of post-operative outcomes, and carries utility for guiding and developing rehabilitation training protocols.



## 1. Introduction

Biomechanical models are frequently used to simulate surgical procedures in order to gain insight into clinical outcomes. For example, computer simulations have been applied to investigate the consequences of muscle re-attachment and tendon transfer procedures in the upper limb (e.g. Giat et al., 1994; Lieber and Friden, 1997; Herrmann and Delp, 1999; De Wilde et al., 2002; Murray et al., 2002, 2006; Saul et al., 2003; Magermans et al., 2004; Veeger et al., 2004; Ling et al., 2009). Biomechanical analysis generally involves calculating factors such as muscle moment arms, muscle force-generating capacity, and the maximum isometric moment-generating capacity following tendon transfer over a functional range of motion for a variety of simulated conditions. Differences in these mechanical parameters that are revealed by simulating and comparing different surgical choices suggest the possibility of optimizing outcomes based on the biomechanical design of the procedure. Overall, biomechanical analyses illustrate the potential for surgical simulation to have a powerful impact on patient care.

Simulations of tendon transfers performed in the upper limb suggest that surgical tensioning of transfers can have an important effect on post-operative strength and range of motion. Basic muscle physiology indicates that muscle force varies with muscle length (Gordon et al., 1966). Because the surgeon controls the intraoperative length at which the donor muscle is sutured to the recipient tendon, it follows that selecting an inappropriate attachment length might

* Corresponding author at: Sensory Motor Performance Program, Rehabilitation Institute of Chicago, 345 E. Superior St., Chicago, IL 60611, USA.
Tel.: +1 312 238 1618; fax: +1 312 238 2208.
*E-mail address:* j-mogk@northwestern.edu (J.P. Mogk).

0021-9290/$ - see front matter © 2010 Elsevier Ltd. All rights reserved.
doi:10.1016/j.jbiomech.2010.11.004

compromise the surgical outcome. For example, the brachioradialis (BR) is often used to restore voluntary hand or wrist function to individuals with cervical spinal cord injury. Previous biomechanical simulations of the BR to flexor pollicis longus (FPL) transfer to restore pinch strength indicated that surgical attachment length impacts the posture in which the transferred BR muscle can generate maximum force (Murray et al., 2006). Similar simulations of the BR to extensor carpi radialis brevis (ECRB) transfer suggested that tensioning dictates the active and passive ranges of wrist motion for a given elbow posture (Murray et al., 2002). In general, both simulation (e.g. Lieber and Friden, 1997) and experimental studies (e.g. Kreulen and Smeulders, 2008) advocate surgical decision-making that optimizes biomechanical output of a transferred muscle as a means to improve tendon transfer outcomes.

One limitation to our current understanding is that the focus has been primarily on the biomechanical properties of a single muscle in the limb: the transferred muscle. One reason for this focus is the limited number of quantitative studies characterizing upper limb strength and function in impaired populations, particularly following tendon transfer. One relatively well-studied outcome is the post-operative performance of the BR-FPL transfer, a procedure that restores lateral pinch function following cervical spinal cord injury (e.g. Waters et al., 1985; Brys and Waters, 1987; Johanson et al., 2006). Experimental data indicate that subjects with BR-FPL tendon transfers achieve significantly lower activation of the transferred BR during maximum effort for lateral pinch than elbow flexion, with a more pronounced deficit in patients with weak elbow extensors (Johanson et al., 2006). Moreover, BR-FPL pinch force increases when the elbow is externally stabilized (Brys and Waters, 1987; Johanson et al., 2006), and following surgery to improve elbow extension strength (Freehafer et al., 1988; Waters et al., 1990). These experimental findings contrast with common assumptions in biomechanical analyses of tendon transfers, including that antagonist muscles have sufficient strength to balance and stabilize proximal joints, and that the transferred muscle can be maximally activated post-operatively.

We developed biomechanical simulations of the tetraplegic upper limb following BR-FPL transfer to examine the influence of upper limb strength on predictions of post-operative BR muscle function. Specifically, the purpose was to investigate the combined effects of varying (i) residual muscle strength in the tetraplegic limb and (ii) surgical attachment length on BR activation and lateral pinch force. Additionally, we evaluated the effectiveness of the surgical simulations to predict post-operative lateral pinch forces produced by subjects with BR-FPL tendon transfers.

## 2. Methods

To evaluate the influence of residual muscle strength in the tetraplegic upper limb on post-operative function of the BR-FPL tendon transfer under different surgical tensioning conditions, we integrated biomechanical simulations with experimental data collected from five individuals with tetraplegia and BR-FPL tendon transfers (Table 1) during maximal lateral pinch force exertions. An existing model of the non-impaired upper limb (Holzbaur et al., 2005) was augmented to incorporate the BR-FPL transfer (Murray et al., 2006) and to enable pinch force calculation (Goehler and Murray, 2010). In addition to the transferred BR muscle, our simulations included eight muscles that often remain under voluntary control following cervical SCI: two wrist extensors (extensor carpi radialis brevis, ECRB, and longus, ECRL), three elbow extensors (all three heads of the triceps, TRI), and three elbow flexors (brachialis, BRA, and both heads of the biceps, BIC). The remaining muscles crossing the wrist and elbow were "paralyzed" by setting their active force-generating capacity to zero. Electrogoniometer and electromyographic (EMG) data describing upper limb posture and activation of the ECRB, BIC, and TRI during lateral pinch served as inputs to the simulations. Each simulation computed the highest BR activation for which neither the elbow nor the wrist flexor moment was larger than the respective joint extensor moment based on the measured co-activation pattern. Simulations were repeated at different strength levels and attachment lengths, as described later. Factors characterizing isometric strength in the upper limb were also quantified from each subject to allow subject-specific scaling of individual simulations (Table 2). For each simulation, EMG and force data describing the activity of the transferred brachioradialis and the subject's resulting pinch strength were used to evaluate how accurately the simulations replicated the experimental measurements.

### 2.1. Experimental data

Similar to the protocol described by Johanson et al. (2006), subjects were seated in their wheelchairs, and positioned with their shoulder abducted (90°) and transversely flexed (30°). Subjects were instructed to maintain a fixed elbow position while generating the maximum pinch force possible. Their ability to maintain the test posture was monitored during each pinch force exertion, as described below. Muscle activation was recorded using fine-wire electrodes inserted into the BR and ECRB muscles, as well as surface electrodes placed over the BIC and TRI muscle groups. EMG data were bandpass-filtered (10–1000 Hz; Motion Lab Systems, Inc., Baton Rouge, LA) and sampled at 2000 Hz, and the root mean square (RMS) of each signal was calculated. The RMS-EMG signals from each muscle were normalized to peak activity, as determined from maximum voluntary contractions. The posture maintained during each pinch force exertion was recorded. Electrogoniometers (Biometrics Ltd., Ladysmith, VA) were attached to record elbow, wrist, and thumb metacarpophalangeal (MCP) joint angles. Prior to use in trial-specific simulations, these data were averaged over a 500 ms window, centered about the peak lateral pinch force value.

The isometric moments produced during maximum effort wrist extension, elbow flexion, and elbow extension were measured using a 6-axis force sensor (ATI Industrial Automation, Apex, NC). A custom cuff was worn to create a point of contact with the force sensor. Joint moment was calculated as the product of the force generated and the distance measured between the point of contact and the joint being tested. For wrist extension, the cuff was worn on the dorsum of the hand, and the distance to the radial styloid was measured. For elbow flexion and extension, the cuff was worn at the wrist and the distance to the lateral epicondyle was measured.

Muscle volume of the transferred BR was measured from each subject via magnetic resonance imaging (MRI) using methods described in detail by Holzbaur et al. (2007a). Briefly, the arm containing the transferred BR was scanned using a 1.5 T MRI scanner (GE Healthcare, Milwaukee, WI). The boundaries of the BR muscle were identified and manually outlined on the axial images. To calculate muscle volume, a three-dimensional polygonal surface of the muscle was constructed from the identified muscle boundaries (3D-Doctor, Able Software Corp., Lexington, MA).

**Table 1**
Subject characteristics[a].

| Patient # | Age at testing | Injury level | International classification[b] | Time post-injury | Time post-surgery | Other tendon transfers? |
|---|---|---|---|---|---|---|
| p1 | 37 | C7, complete | OCu-4 | 4 y, 3 mo | 1 y, 5 mo | ECRL-FDP, and opponensplasty |
| p2[c] | 56 | C6–C7, incomplete | | 24 y | 22 y | |
| p3 | 57 | C4–C7, complete | OCu-5 | 33 y, 6 mo | 17 y, 2 mo | ECRL-FDP, and Zancolli lasso |
| p4 | 29 | C6, complete | OCu-5 | 3 y, 8 mo | 1 y, 2 mo | ECRL-FDP, split FPL-EPL, and CMC joint fusion |
| p5 | 50 | C6–C7, complete | OCu-5 | 4 y | 1 y, 2 mo | ECRL-FDP, split FPL-EPL, and CMC joint fusion |

[a] All subjects in this study were male.

[b] The International Classification of Surgery of the Hand in Tetraplegia (ICSHT) was devised to categorize patients according to the sensory and motor characteristics of the upper limb (McDowell et al., 1986). This scheme characterizes limb sensibility as ocular (O, possessing visual afferent feedback) and/or cutaneous (Cu, having a minimum two-point discrimination of 10 mm within the thumb and index finger pulp). Patients are also categorized by the number of muscles below the elbow with at least Grade 4 strength (i.e. strength is reduced but muscle contraction can move the joint against resistance).

[c] Details for this individual's International Classification, and whether he had any other transfer surgeries are unknown since his surgery was performed at a different facility than where the testing occurred.

**Table 2**
Summary of experimentally measured data.

| Patient # | BR volume ($cm^3$)[a] | Elbow flexion ($N \cdot m$)[a] | Elbow extension ($N \cdot m$)[a] | Wrist extension ($N \cdot m$)[a] | # of pinch force trials[b] | BIC activation[c] | TRI activation[c] | ECRB activation[c] | BR activation[d] | Pinch force (N)[d] |
|---|---|---|---|---|---|---|---|---|---|---|
| p1 | 85.5 | 38.6 | 28.0 | 3.4 | 3 | 0.274 (0.022) | 0.518 (0.009) | 0.979 (0.036) | 0.371 (0.015) | 35.4 (2.0) |
| p2 | 62.2 | 34.7 | 17.6 | 7.7 | 3 | 0.175 (0.013) | 0.762 (0.036) | 0.052 (0.030) | 0.276 (0.026) | 22.7 (0.5) |
| p3 | 69.4 | 31.5 | 19.2 | 2.6 | 3 | 0.269 (0.160) | 0.686 (0.038) | 0.743 (0.021) | 0.393 (0.045) | 22.4 (1.3) |
| p4 | 58.4 | 31.5 | 14.7 | 4.7 | 2 | 0.536 (0.036) | 0.832 (0.011) | 0.540 (0.007) | 0.542 (0.021) | 20.9 (2.6) |
| p5 | 63.2 | 28.4 | 22.0 | 2.3 | 3 | 0.357 (0.066) | 0.340 (0.030) | 0.666 (0.071) | 0.408 (0.030) | 11.7 (1.2) |

[a] BR muscle volume and joint strength data were used to scale muscle strength for each of the patient-specific strength models.
[b] Simulations were performed using trial-specific data, but the values presented in the proceeding columns indicate the mean ($\pm$SD) of the measured data across trials for each subject that was simulated.
[c] Measured co-activation patterns of the BIC, TRI, and ECRB were used to drive simulations.
[d] Measured BR activation and pinch force magnitude were compared to simulation outputs to evaluate performance.

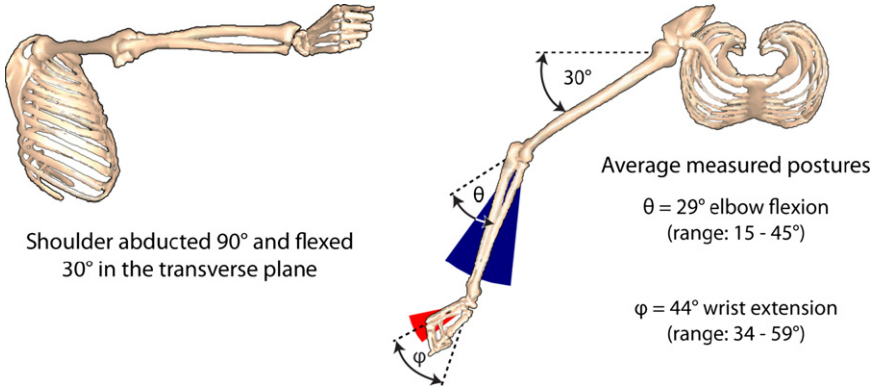


**Fig. 1.** Goniometric data for the elbow, wrist, and thumb MCP joints were used to constrain the solutions to measured postures. The shoulder was abducted 90° and flexed 30° in the transverse plane, based on the experimental test configuration (Johanson et al., 2006). Note that all simulations reflected relatively extended wrist and elbow postures, based on the average postures measured from the five individuals during maximal lateral pinch force efforts.

### 2.2. Computer simulations

Following transfer to the FPL, brachioradialis acts to flex the elbow, wrist, and thumb joints during lateral pinch effort. Each simulation computed the highest BR activation ($act^{BR}$) for which neither the elbow nor the wrist flexor moment was larger than the respective joint extensor moment based on the measured co-activation pattern. That is,

$$M^{elbow}_{BR-FPL} + M^{elbow}_{BIC} + M^{elbow}_{BRA} + M^{elbow}_{ECRB} + M^{elbow}_{ECRL} + M^{elbow}_{passive} \le M^{elbow}_{TRI} \quad (1)$$

$$M^{wrist}_{BR-FPL} + M^{wrist}_{passive} \le M^{wrist}_{ECRB} + M^{wrist}_{ECRL} \quad (2)$$

where $M^{joint}_{muscle}$ is the moment produced by a given muscle about the specified joint, and $M^{joint}_{passive}$ includes posture-dependent inertial moments and passive moments produced by the paralyzed muscles. Thus, $act^{BR}$ (ranging from 0 to 1) defines the fraction of posture-specific active BR muscle force that could be exerted without generating a net flexion moment at either joint. Joint moments were balanced about the flexion–extension axes only. The lateral pinch force produced by the transferred BR was estimated by transforming the muscle force produced by the BR-FPL transfer, based on the calculated activation level, to the endpoint force at the thumb-tip (Goehler and Murray, 2010).

To solve the moment balance equations, we developed a program in MATLAB (The MathWorks, Inc., Natick, MA) in which experimentally recorded joint angles and EMG co-activation patterns for the BIC, TRI, ECRB served as inputs, and $act^{BR}$ and lateral pinch force were outputs. For a given simulation, normalized EMG data recorded from the BIC, TRI, and ECRB were used to define the activation levels of the modeled elbow flexors, as well as elbow and wrist extensors, respectively (Table 2). The moment arms, musculotendon lengths, active and passive isometric force- and moment-generating properties of the BR-FPL transfer and the upper limb muscles were defined as described previously (Holzbaur et al., 2005; Murray et al., 2006), except for the tendon stress–strain relationships defined for the ECRB and ECRL, which were adapted using experimentally determined biomechanical tendon properties (Loren and Lieber, 1995). We incorporated passive properties for the transferred BR muscle as determined *in vivo* by Lieber et al. (2005), with passive force initiated at optimal fiber length ($\ell^M_o$). Activation-dependent scaling of $\ell^M_o$, and fiber length-dependent changes in pennation angle, were incorporated for all active muscles (c.f. Lloyd and Besier, 2003). Joint postures were constrained to measured elbow, wrist and thumb metacarpophalangeal (MCP) joint postures, and the fingers loosely flexed (Fig. 1).

For each subject, simulations were repeated for two different strength levels ("non-impaired" and "patient-specific"), at each of two tendon attachment lengths, for each experimental trial (4 simulations were performed for each of the 14 trials of experimental data). "Non-impaired strength" assumed healthy muscle volumes (Holzbaur et al., 2007a), and thus force- and moment-generating capacity, in the tetraplegic upper limb. "Patient-specific strength" adjusted the maximum isometric muscle force- and moment-generating capacity in the model to represent individual subjects using a combination of the patient-specific wrist and elbow torque measurements and BR volume data measured via MRI. Patient-specific strength models used individually imaged BR muscle volume ($vol^{BR}$) to calculate peak isometric BR muscle force ($F^{BR}_o$) according to:

$$F^{BR}_o = \frac{vol^{BR}}{\ell^{BR}_o}\sigma \quad (3)$$

where $\ell^{BR}_o$ is the optimal BR fiber length from the model and $\sigma$ the specific muscle tension used for all muscles (50.8 $N/cm^2$). Specific muscle tension was calculated from previous studies, by identifying the best fit between the average muscle volume data for 5 healthy young males (Holzbaur et al., 2007a), and joint moments measured from the same 5 individuals (Holzbaur et al., 2007b). Maximum isometric muscle force ($F^M_o$) for the remaining eight muscles was scaled from non-impaired values based on posture-specific wrist and elbow strength measured from each individual with tetraplegia and the BR-FPL transfer (Fig. 2). The maximum isometric muscle forces used for each simulated strength condition, expressed as a proportion of the non-impaired model, are summarized in Table 3.

We simulated two surgical attachment lengths by adjusting the modeled BR-FPL tendon slack length to place the transferred BR (i) at its natural *in situ* length for the transfer posture (termed "resting" tension), and (ii) at 80% of *in situ* length ("loose" tension) (Murray et al., 2006).

Repeated measures ANOVAs and post-hoc comparisons were performed to evaluate the effects of modeled strength (non-impaired, and patient-specific strength) and surgical tensioning (loose and resting) on $act^{BR}$ and lateral pinch force magnitude. Significance was set at $p=0.01$. Root mean square error (RMSE)

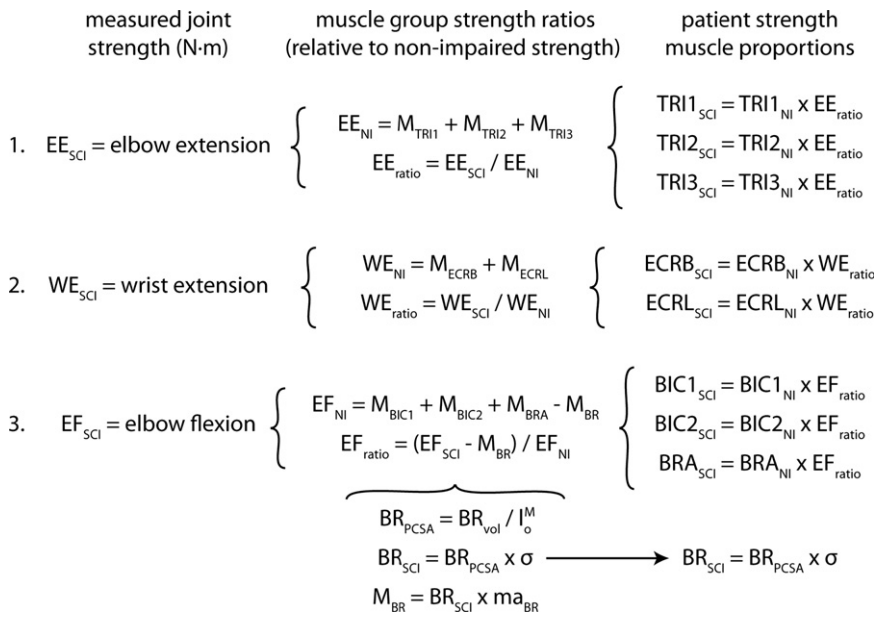


**Fig. 2.** Schematic of the process followed to compute muscle forces for each of the personalized patient-specific strength models. Strength ratios were calculated for each patient, relative to the non-impaired (NI) strength model, and used to scale the maximum isometric force of (1) the three heads of the triceps (TRI1, TRI2, and TRI3), (2) the two wrist extensors (ECRB and ECRL), and (3) the two heads of the biceps (BIC1 and BIC2) and brachialis (BRA) muscles. Strength was computed as the sum of posture-specific muscle moments (M) generated by each muscle group, assuming full agonist muscle activation, and zero antagonist co-activation. Note the elbow flexors were scaled based on a combination of measured joint strength and imaged volume of the BR muscle.

**Table 3**
Summary of the relative maximum muscle force proportions of the non-paralyzed arm muscles used in the tetraplegic upper limb model.

| Modeled strength | Non-paralyzed muscles included in the tetraplegic upper limb model | | | |
|---|---|---|---|---|
| | BR-FPL | BIC (both heads) and BRA | TRI (all 3 heads) | ECRB and ECRL |
| Non-impaired | 1 | 1 | 1 | 1 |
| Patient 1 | 0.880 | 0.602 | 0.874 | 0.245 |
| Patient 2 | 0.601 | 0.511 | 0.458 | 0.394 |
| Patient 3 | 0.640 | 0.566 | 0.548 | 0.589 |
| Patient 4 | 0.714 | 0.493 | 0.599 | 0.209 |
| Patient 5 | 0.650 | 0.443 | 0.686 | 0.171 |
| Average patient[a] | 0.697 | 0.523 | 0.633 | 0.322 |

[a] Average patient strength muscle force proportions are reported to indicate the average force-generating capacity of these muscles, in the patient cohort studied, in relation to non-impaired strength muscles.

was calculated for each simulated condition to evaluate how well experimentally measured lateral pinch force and BR activation were predicted by modeled combinations of muscle strength and BR-FPL tensioning.

## 3. Results

Both the level to which the transferred brachioradialis could be activated and the lateral pinch force it produced varied with modeled muscle strength. Using each subject's experimentally recorded co-activation pattern, the simulations that incorporated non-impaired strength generally produced the highest BR activation and the largest pinch force (Fig. 3). Using non-impaired strength, the co-activation patterns from four of the five individuals studied supported maximum activation of the transferred BR and comparable levels of pinch force (Fig. 3A and C). Interestingly, the co-activation patterns from the fifth subject generated a net elbow flexion moment even when the transferred BR was not activated. Thus, these simulations predicted no BR activation ($act^{BR}=0$), and the resultant pinch forces arose from the passive BR-FPL force–length properties. When the same five sets of co-activation patterns served as inputs to simulations that incorporated patient-specific strength, we observed increased variability of BR activation and decreased pinch forces (Figs. 3B and D; $p=0.0019$). Unlike the non-impaired simulations, the co-activation patterns from the fifth subject supported active BR function, although BR activation was minimal ($\sim$20% of maximum) in the patient-specific simulations. Excluding the unique co-activation patterns of the fifth subject, pinch forces decreased by $38.4 \pm 18.5\%$ (mean $\pm$ SD) using patient-specific strength.

The effect of surgical tensioning of the BR-FPL tendon transfer on BR activation and lateral pinch force was also highly dependent on simulated muscle strength. Loose tensioning of the BR-FPL transfer in the non-impaired strength model augmented lateral pinch force by an average of $61.6 \pm 86.5\%$ ($p<0.001$; Fig. 4A; $101.5 \pm 39.5\%$ increase without the simulations for the fifth subject). The pinch force increased due to the greater active isometric force that the BR muscle could produce at the shorter fiber lengths (Fig. 4B), combined with nearly maximal BR activation for co-activation patterns from four of five subjects (Fig. 4C). Pinch forces remained passive for loose tensioning using the co-activation patterns of the fifth subject, but decreased to less than 2 N, since lower passive force developed at the shorter fiber length. In contrast, loose tensioning in the patient-specific strength models did not significantly alter lateral pinch force ($p=0.19$), despite the identical shift in fiber length (Fig. 4). Pinch force did not increase in patient-specific strength models because, as with resting tensioning, the transferred BR could only be submaximally activated before generating a net flexion moment about one (or both) of the proximal joints.

The simulations that incorporated patient-specific strength generally reflected the experimental data better than the non-impaired

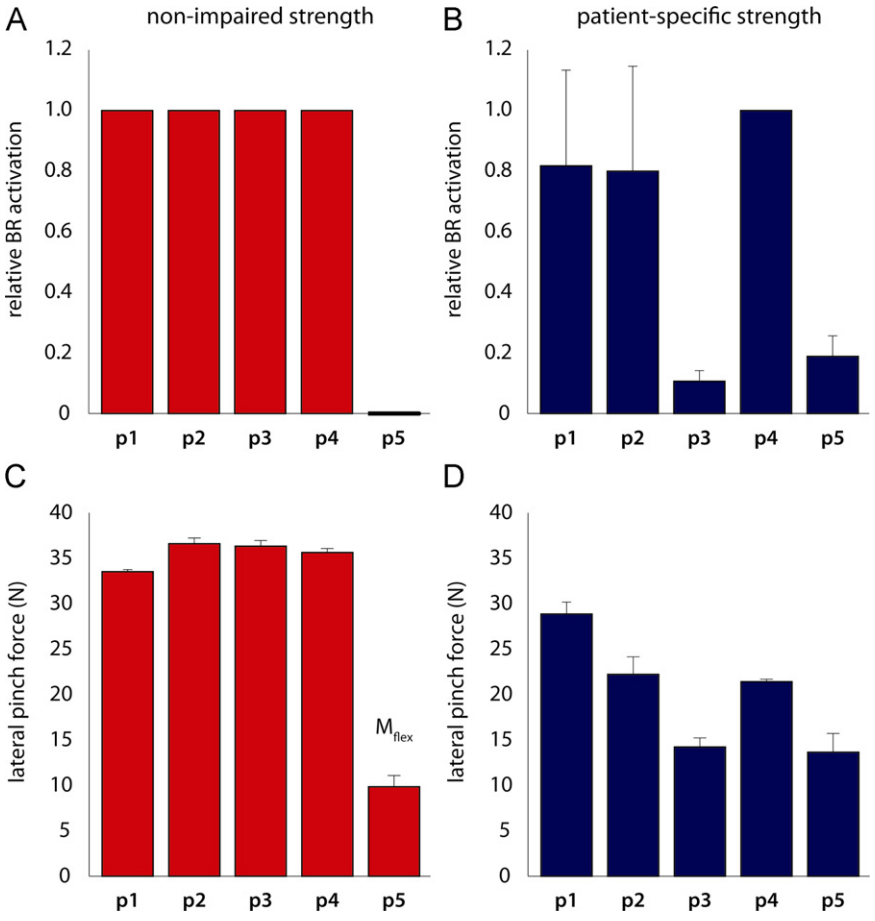


**Fig. 3.** (A and B) Relative activation of the transferred BR muscle and (C and D) absolute lateral pinch force (in Newtons) predicted by simulations incorporating non-impaired, and patient-specific strength, based on the muscle co-activation patterns recorded from each patient (3 trials for four of five patients, and 2 trials for the final patient; 14 trials in total). (A) Non-impaired strength enabled maximum BR activation for co-activation patterns measured from four of five individuals studied, but zero activation for the fifth (p5), leading to (C) relatively consistent pinch force magnitudes for all but one individual, whose co-activation patterns generated a net flexion moment even without activation of the transferred BR. (B) Patient-specific strength increased variability in BR activation, and thus (D) pinch force magnitudes across subjects. $M_{flex}$ indicates co-activation patterns, which could not support BR activation without generating a net elbow flexion moment, and thus entirely passive lateral pinch forces. All of the results presented here are for the "resting" tensioning condition.

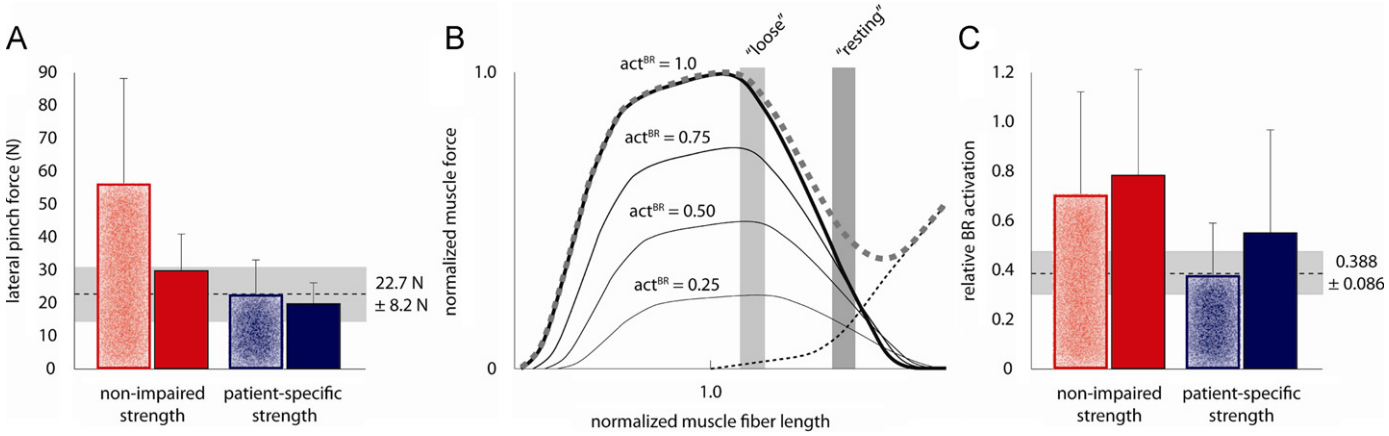


**Fig. 4.** The effect of "loose" and "resting" surgical tensioning (speckled and solid bars, respectively) on (A) the predicted lateral pinch force magnitude, (B) where the transferred BR muscle would operate on the force–length relationship for the postures studied, and (C) the corresponding BR activation for each of the modeled muscle strength conditions. The broken horizontal line specifies the mean (A) pinch forces and (C) BR activation ( ± SD in light grey, 14 total trials for each condition) experimentally measured from the five individuals studied who had received the BR-FPL transfer. (B) Vertical bars indicate the range of fiber lengths for the transferred BR muscle, and the corresponding muscle force that could be generated at specific levels of BR activation, based on the postures measured during lateral pinch force efforts.

strength simulations. Overall, non-impaired strength simulations predicted significantly higher BR activation ($p=0.0052$) and pinch force magnitudes ($p=0.0063$) than were experimentally measured. Regardless of tensioning, the patient-specific strength simulations yielded smaller errors than the simulations involving non-impaired strength (Table 4).

**Table 4**
Root mean square error (RMSE) calculated between simulation results and experimental data.

| Modeled muscle strength conditions | BR activation | | Lateral pinch force (N) | |
|---|---|---|---|---|
| | "loose" (80% *in situ*) | "resting" (100% *in situ*) | "loose" (80% *in situ*) | "resting" (100% *in situ*) |
| Non-impaired[a] | 0.516 | 0.585 | 42.3 | 10.8 |
| Patient-specific[b] | $0.189 \pm 0.153$ | $0.417 \pm 0.155$ | $7.4 \pm 5.5$ | $4.2 \pm 3.1$ |

[a] A single RMSE value was calculated for each of the modeled strength levels. Consequently, a single RMSE value is presented for the simulations performed using the non-impaired strength model.
[b] The average RMSE ($\pm$ SD) is presented for the simulations performed using the five personalized, patient-specific strength models.

## 4. Discussion

A biomechanical model of the tetraplegic upper limb following BR-FPL transfer was used to examine how the level of residual active muscle strength in the tetraplegic limb influences post-operative function of the transferred muscle. Simulations revealed that as residual extensor muscle strength was decreased, so too was the potential to generate active pinch force using a given co-activation pattern. By incorporating patient-specific muscle weakness and imbalance into the model, the potential to enhance pinch force through surgical tensioning became restricted. Importantly, incorporating patient-specific muscle volume, EMG activity, joint posture, and strength measurements led to simulation results that were comparable to post-operatively measured BR activation and pinch force magnitude. These results demonstrate the importance of gathering data to scale models appropriately so that simulations behave in accordance with the population of interest.

Simulations indicated that, for a given coordination pattern, extensor muscle weakness restricted the level of BR activation and resultant pinch force possible. For resting tensioning, non-impaired extensor strength was sufficient to balance the wrist and elbow joints against maximum BR activation for co-activation patterns recorded from four of five individuals (Fig. 3). However, even with non-impaired strength, coordination patterns also existed that severely limited BR activation for lateral pinch (p5 in Fig. 3). Specifically, the elbow extensor activity recorded from one individual was insufficient to balance the elbow and support active pinch force, highlighting that the ability to activate and effectively coordinate the residual muscles in the tetraplegic upper limb is necessary during lateral pinch, even when subjects possess adequate strength. Weakening the model to patient-specific strength further increased the sensitivity of simulations to muscle coordination patterns, reducing BR activation and pinch force uniquely for the co-activation patterns adopted by different subjects (Fig. 3). Note that we examined the outputs generated by different strength models using the same coordination patterns as input. In general, simulations showed that the weaker the model, the more a given coordination pattern limited post-operative performance. Future use of optimization to determine optimal coordination patterns, which generate the largest force output while maintaining wrist and elbow joint balance, could be used to inform rehabilitation strategies or establish goals for training protocols. Our results suggest that such use of the model requires accurate assessment of patient-specific muscle strength.

Extensor muscle weakness diminished the potential to alter the total pinch force output using surgical tensioning; however, the ability to influence the relative active force contribution through tensioning persisted. In our simulations, loose tensioning shifted the transferred BR to operate at shorter fiber lengths, and effectively doubled the force-generating capacity of the BR-FPL transfer for the extended postures adopted by the subjects during testing (Fig. 4B). For simulations that incorporated non-impaired strength, pinch force increased by more than 60% over resting tensioning (Fig. 4), and doubled when passive results from patient 5 simulations were excluded. In contrast, simulations that incorporated patient-specific strength attenuated the potential pinch force enhancement through tensioning to approximately 10% (Fig. 4). Limited by extensor strength, the patient-specific models responded to the decreased passive force component by increasing the relative active force contribution, while the total force (active plus passive) produced by the BR-FPL transfer remained constant. Patient-specific simulations suggest that it would be difficult to use tensioning to optimize pinch force magnitude, but could still be used to improve active control of pinch force when the extensor muscles are weak.

In this study, we evaluate the interplay between surgical tensioning and extensor strength in an extended limb posture. Muscle strength varies with posture (e.g. Mogk and Keir, 2003), and the effects of surgical tensioning are also thought to depend on limb posture (Murray et al., 2006). We expect that adequate extensor strength is necessary for optimal performance of the BR-FPL transfer in all upper limb postures, although we only highlight results for a single posture here.

This simulation study demonstrates the importance of considering the strength of the impaired limb when using a biomechanical model to predict outcomes following tendon transfer surgery. Our simulations replicate conventional clinical wisdom that the elbow extensors must possess adequate residual function, or be surgically supplemented, to optimize post-operative outcomes of BR-FPL transfers (Waters et al., 1985, 1990; Brys and Waters, 1987; Johanson et al., 2006). Our results suggest that the influence of the biomechanical properties of an individual transferred muscle on clinical outcomes is subtler in the weakened upper limb than it would be in a limb with greater strength. This study provides additional evidence of the importance of developing rehabilitation interventions that improve proximal strength in order to improve hand function in the tetraplegic upper limb.

## Conflict of interest statement

The authors of this manuscript have no financial or personal relationships with any people or organizations that could inappropriately influence the work presented.

## Acknowledgements

This work was funded by NIH 5 R01 HD 046774 and VA A3741R.

## References

Brys, D., Waters, R.L., 1987. Effect of triceps function on the brachioradialis transfer in quadriplegia. Journal of Hand Surgery 12A, 237–239.
De Wilde, L., Audenaert, E., Barbaix, E., Audenaert, A., Soudan, K., 2002. Consequences of deltoid muscle elongation on deltoid muscle performance: a computerised study. Clinical Biomechanics 17, 499–505.

Freehafer, A.A., Peckham, P.H., Keith, M.W., Mendelson, L.S., 1988. The brachioradialis: anatomy, properties, and value for tendon transfer in the tetraplegic. Journal of Hand Surgery 13A, 99–104.

Giat, Y., Mizrahi, J., Levine, W.S., Chen, J., 1994. Simulation of distal tendon transfer of the biceps brachii and the brachialis muscles. Journal of Biomechanics 27, 1005–1014.

Goehler, C.M., Murray, W.M., 2010. The sensitivity of endpoint forces produced by the extrinsic muscles of the thumb to posture. Journal of Biomechanics 43, 1553–1559.

Gordon, A.M., Huxley, A.F., Julian, F.J., 1966. The variation in isometric tension with sarcomere length in vertebrate muscle fibres. Journal of Physiology 184, 170–192.

Herrmann, A.M., Delp, S.L., 1999. Moment arm and force-generating capacity of the extensor carpi ulnaris after transfer to the extensor carpi radialis brevis. Journal of Hand Surgery 24A, 1083–1090.

Holzbaur, K.R., Murray, W.M., Delp, S.L., 2005. A model of the upper extremity for simulating musculoskeletal surgery and analyzing neuromuscular control. Annals of Biomedical Engineering 33, 829–840.

Holzbaur, K.R., Murray, W.M., Gold, G.E., Delp, S.L., 2007a. Upper limb muscle volumes in adult subjects. Journal of Biomechanics 40, 742–749.

Holzbaur, K.R., Delp, S.L., Gold, G.E., Murray, W.M., 2007b. Moment-generating capacity of upper limb muscles in healthy adults. Journal of Biomechanics 40, 2442–2449.

Johanson, M.E., Hentz, V.R., Smaby, N., Murray, W.M., 2006. Activation of brachioradialis muscles transferred to restore lateral pinch in tetraplegia. Journal of Hand Surgery 31A, 747–753.

Kreulen, M., Smeulders, M.J., 2008. Assessment of flexor carpi ulnaris function for tendon transfer surgery. Journal of Biomechanics 41, 2130–2135.

Lieber, R.L., Friden, J., 1997. Intraoperative measurement and biomechanical modeling of the flexor carpi ulnaris-to-extensor carpi radialis longus tendon transfer. Journal of Biomechanical Engineering 119, 386–391.

Lieber, R.L., Murray, W.M., Clark, D.L., Hentz, V.R., Friden, J., 2005. Biomechanical properties of the brachioradialis muscle: implications for surgical tendon transfer. Journal of Hand Surgery 30A, 273–282.

Ling, H.Y., Angeles, J.G., Horodyski, M.B., 2009. Biomechanics of latissimus dorsi transfer for irreparable posterosuperior rotator cuff tears. Clinical Biomechanics 24, 261–266.

Lloyd, D.G., Besier, T.F., 2003. An EMG-driven musculoskeletal model to estimate muscle forces and knee joint moments in vivo. Journal of Biomechanics 36, 765–776.

Loren, G.J., Lieber, R.L., 1995. Tendon biomechanical properties enhance human wrist muscle specialization. Journal of Biomechanics 28, 791–799.

Magermans, D.J., Chadwick, E.K., Veeger, H.E., Rozing, P.M., van der Helm, F.C., 2004. Effectiveness of tendon transfers for massive rotator cuff tears: a simulation study. Clinical Biomechanics 19, 116–122.

McDowell, C.L., Moberg, E.A., House, J.H., 1986. The 2nd international-conference on surgical rehabilitation of the upper limb in tetraplegia (quadriplegia). Journal of Hand Surgery 11A, 604–608.

Mogk, J.P., Keir, P.J., 2003. The effects of posture on forearm muscle loading during gripping. Ergonomics 46, 956–975.

Murray, W.M., Bryden, A.M., Kilgore, K.L., Keith, M.W., 2002. The influence of elbow position on the range of motion of the wrist following transfer of the brachioradialis to the extensor carpi radialis brevis tendon. Journal of Bone and Joint Surgery 84A, 2203–2210.

Murray, W.M., Hentz, V.R., Friden, J., Lieber, R.L., 2006. Variability in surgical technique for brachioradialis tendon transfer. Evidence and implications. Journal of Bone and Joint Surgery 88A, 2009–2016.

Saul, K.R., Murray, W.M., Hentz, V.R., Delp, S.L., 2003. Biomechanics of the Steindler flexorplasty surgery: a computer simulation study. Journal of Hand Surgery 28A, 979–986.

Veeger, H.E., Kreulen, M., Smeulders, M.J., 2004. Mechanical evaluation of the Pronator Teres rerouting tendon transfer. Journal of Hand Surgery 29B, 259–264.

Waters, R., Moore, K.R., Graboff, S.R., Paris, K., 1985. Brachioradialis to flexor pollicis longus tendon transfer for active lateral pinch in the tetraplegic. Journal of Hand Surgery 10A, 385–391.

Waters, R.L., Stark, L.Z., Gubernick, I., Bellman, H., Barnes, G., 1990. Electromyographic analysis of brachioradialis to flexor pollicis longus tendon transfer in quadriplegia. Journal of Hand Surgery 15A, 335–339.